A precise correcting method for the study of the superhard material using nanoindentation tests

Yan Ping Cao
Laboratoire des Systèmes Mécaniques et d'ingénierie Simultanée, Université de Technologie de Troyes, 10010 Troyes, France; and Forschungszentrum Karlsruhe, Institut für Materialforschung II, D-76344 Eggenstein-Leopoldshafen, Germany

Ming Dao
Department of Materials Science and Engineering, Massachusetts Institute of Technology, Cambridge, Massachusetts 02139

Jian Lu[a)]
Department of Mechanical Engineering, Hong Kong Polytechnic University, Hung Hom, Kowloon, Hong Kong

The accurate description of the indentation load–displacement relationship of an elastic sharp indenter indenting into an elastic half-space is critical for analyzing the nanoindentation data of superhard materials using the procedure proposed by Oliver and Pharr [*J. Mater. Res.* **7,** 1564 (1992)]. A further discussion on this issue is made in the present work to reconcile the apparent inconsistencies that have appeared between the experimental results reported by Lim and Chaudhri [*Philos. Mag.* **83,** 3427 (2003)] and the analysis performed by Fischer-Cripps [*J. Mater. Res.* **18,** 1043 (2003)]. It is found that the indenter size effect is responsible for this large discrepancy. Moreover, according to our analysis, we found that when the deformation of the indenter is significant, besides the errors caused by the Sneddon's boundary condition as addressed by Hay et al. [*J. Mater. Res.* **14,** 2296 (1999)], the errors induced by the application of reduced modulus should be considered at the same time in correcting the modified Sneddon's solution. In the present work, for the diamond indenter of 70.3° indenting into an elastic half-space with its Poisson's ratio varying from 0.0 to 0.5 and the ratio of the Young's modulus of the indented material to that of the diamond indenter, $E_{material}/E_{indenter}$, varying from 0 to 1, a set of new correction factors are proposed based on finite element analysis. The results reported here should provide insights into the analysis of the nanoindentation load–displacement data when using a diamond indenter to determine the hardness and Young's modulus of superhard materials.

I. INTRODUCTION

During the past 3 decades, depth sensing instrumented indentation tests have become an important tool to determine the mechanical properties of materials at different length scales (e.g., nanometer and micrometer scales). Using indentation tests, Young's modulus and hardness can be measured following the method of Doerner and Nix[1] or Oliver and Pharr.[2] It is also possible to use indentation tests to determine the stress–strain curves of elastoplastic materials.[3–15] Besides being used on bulk materials, indentation tests can be used to probe the mechanical properties of thin films and coating systems.[16,17] The present research is relevant for the analysis of the conical indentation into an elastic half-space, which is useful when taking at least the following two aspects into consideration. First, there indeed exist materials that exhibit elastic deformation under indentation (e.g., rubber-like materials and some superhard materials). Second, the solution of the indentation into an elastic half-space forms the basis of analyzing the nanoindentation data by using the classic method of Oliver and Pharr.[2] Giannakopoulos et al.[18] and Larsson et al.[19] explored the Vickers and Berkovich indentation into an elastic half-space by using finite element computations. Hay et al.[20] examined the Sneddon's solution[21] by analyzing the conical indentation of linearly elastic

materials. In their analysis,[18–20] the indenter was assumed to be rigid. However, in the nanoindentation of superhard materials, which is the main concern of the present research, the indenter can undergo significant elastic deformation. To include the effect of the indenter compliance, a common practice of so-called reduced modulus was used in the method of Oliver and Pharr.[2] There have recently been a few conflicting reports[21–24] regarding the applicability of the reduced modulus, as described in detail below in this section.

In the procedure proposed by Oliver and Pharr,[2] a key relation is applied to relate the indentation response to the material properties for the case of conical indentation

$$S = \frac{2}{\sqrt{\pi}} E^* \sqrt{A} \quad , \tag{1}$$

where S, A are the contact stiffness and the contact area, respectively. E^* is the reduced modulus which is given by

$$\frac{1}{E^*} = \frac{1 - \nu^2}{E} + \frac{1 - \nu_i^2}{E_i} \quad , \tag{2}$$

where E and ν are the Young's modulus and Poisson's ratio of the elastic solids, respectively, and E_i and ν_i are the Young's modulus and Poisson's ratio of the elastic indenter, respectively. The relation comes from the elastic-contact analysis and specially the modified Sneddon's solution[2] for conical indentation

$$P = \frac{2}{\pi} E^* \tan(\theta) h^2 \quad , \tag{3}$$

where P, h, and θ are the indentation load, the indentation depth, and the half-apex angle of the indenter, respectively. Equation (3) is an extension of the original Sneddon's solution[25] for a rigid conical indenter, that is

$$P = \frac{2}{\pi} \frac{E}{1 - \nu^2} \tan(\theta) h^2 \quad . \tag{4}$$

Up to now, no rigorous theoretical proof has been provided for the extension of Eq. (4) to Eq. (3). Chaudhri[21] pointed out that such an extension is questionable when the deformation of the indenter is significant. However, the numerical and theoretical analysis performed by Fischer-Cripps[22] showed that the application of Eq. (3) using reduced Young's modulus in nanoindentation tests can provide reliable results for the determination of hardness and Young's modulus. Recently, Lim and Chaudhri[23] carried out comprehensive experiments to verify the effectiveness of Eq. (3). Based on their results, Lim and Chaudhri[23] suggested that when the Young's modulus of the indented material is comparable with that of the indenter, the modified Sneddon's solution[2] is no longer valid, which is apparently inconsistent with the numerical results of Fischer-Cripps.[22] Lim and

Chaudhri[23] also argued that if the indenter with the half-apex angle of 75° is applied, the Sneddon's solution given by Eq. (4) instead of Eq. (3) should be applied to extract mechanical properties of indented materials. Accordingly, they suggested revised values of the Young's modulus, which are much smaller than the originally reported values, for several superhard materials that had been reported in the literature.[26–29]

The main intention of the present work is to reconcile the apparent inconsistencies found in the literature and to further examine the errors induced by the application of the so-called reduced modulus when the indenter exhibits significant elastic deformation. We start from the interesting experiments designed by Lim and Chaudhri[23] by simulating a rubber indenter indenting into a rubber half-space (see Sec. II). The subsequent analysis (see Sec. III) aims at revealing the reason why the load–depth curves in the experiments[23] are far from the results given by the theoretical and numerical analysis.[22] In Sec. IV, the performance of Eq. (3) in the analysis of nanoindentation into superhard materials is further examined by simulating a diamond indenter indenting into an elastic half-space considering different elastic properties. The analysis shows that corrections to Eq. (3) are needed and are proposed in the present research for a specific conical indenter. Section V summarizes the main findings in the present work.

II. SIMULATIONS OF THE EXPERIMENTS PERFORMED IN THE LITERATURE

The experiments performed by Lim and Chaudhri[23] using a conical indenter with a half-apex angle of 75° were simulated by applying ABAQUS,[30] a general purpose commercial finite element software. The objective is to confirm the large discrepancy between the experimental results[23] and the results from theoretical and numerical analysis.[22] Figure 1 shows the schematic of the indenter and the indented material. By referring to the experiments of Lim and Chaudhri,[23] the radius R_w and the height L_h of the substrate for the rubber block, PDMS (1:10) and soda-lime glass block are taken as 36 mm × 40 mm, 14 mm × 25 mm, and 36 mm × 25 mm, respectively. The material properties of the indenter and the indented materials in the work of Lim and Chaudhri[23] were used in the present simulations (see Table I for detail). An axisymmetric model was adopted, and a total of 10,000 four-node bilinear axisymmetry elements was used to model the semi-infinite substrate of the indented solid. Figure 2 is the mesh of the rubber indenter indenting into the rubber block. A mesh similar to that shown in Fig. 2 is used for other cases. It should be pointed out that the 75° indenter has a tip radius of 0.28 mm,[23] which is also simulated in the present analysis. The boundary conditions on the indented solid were specified such that the
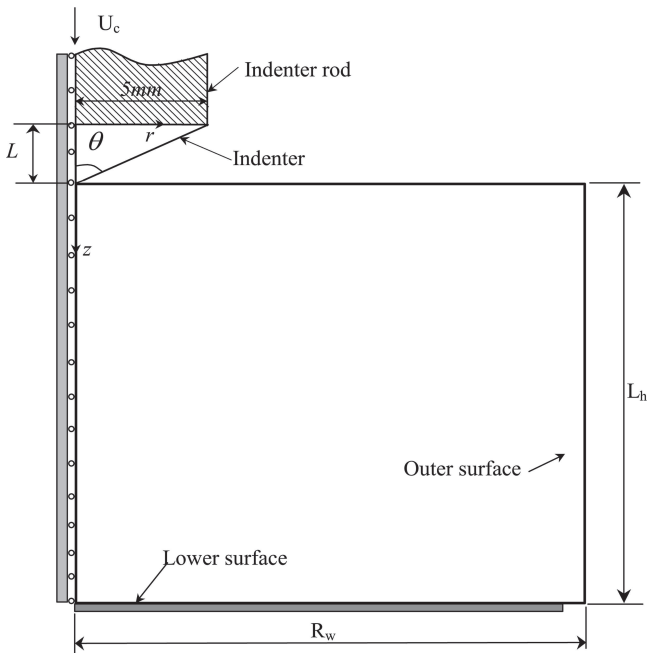
FIG. 1. A schematic drawing of the computational model (an elastic conical indenter indenting into an elastic solid) used in the present analysis.

TABLE I. Material properties used in the simulation of the experiments performed by Lim and Chaudhri.[23]

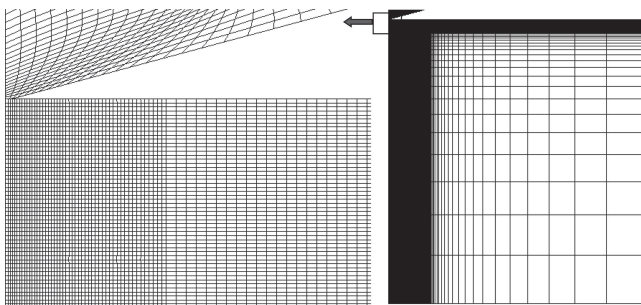| Materials	Young's modulus (MPa)	Poisson's ratio
Rubber conical indenter	2.45	0.5
Rubber block	2.45	0.5
PDMS (1:10)	1.5	0.5
Soda-lime glass	70,000	0.25

FIG. 2. Finite element mesh used in the present analysis.

outer-surface nodes are traction-free with fixed lower-surface nodes, as given by Fig. 1, and the following equations

$$T_r(r = R_w) = 0, \ T_z(r = R_w) = 0 \quad \text{(outer surface)} \quad , \quad (5)$$

and

$$U_r(z = L_h) = 0, \ U_z(z = L_h) = 0 \quad \text{(lower surface)} \quad , \quad (6)$$

where T represents the traction force, and U represents the displacement. It is assumed that the machine compliance has already been excluded from the recorded displacement. Considering that the indenter rod is made of aluminum,[23] the Young's modulus of which is much larger than that of rubber, the aluminum rod is assumed to be rigid. The rigid indenter rod was assumed to be well-bonded with the indenter; in the simulation this was realized by assuming that the upper surface of the indenter has a finite displacement U_c in the direction z, which is the same as that of the indenter rod, and no displacement was seen in the direction r. In equation form, they are expressed as

$$U_{r,\text{upper}} = 0$$
$$U_{z,\text{upper}} = U_{z,\text{rod}} = U_c \quad . \quad (7)$$

In this case, a displacement-controlled loading procedure is applied. Friction was omitted here, according to Mata and Alcalá.[12] In the simulations, the indenter and the indented materials were both assumed to be linearly elastic, and large deformation formulations were adopted.[20] The computational results and corresponding experimental results are given in Fig. 3. In Fig. 3, the indentation depth is the displacement of the indenter rod and also the upper surface of the indenter in the loading direction. The maximum indentation depth is obtained by referring to that in the experiments of Lim and Chaudhri.[23] The analysis performed by Fischer-Cripps,[22] however, showed that the modified Sneddon's solution given by Eq. (3) (the dotted lines in Fig. 3) still works very well, even where the deformation of the indenter is significant. Therefore, from the results in Fig. 3, it can be seen that the present computational results agree well with the experiments,[23] and these results computationally reproduce the large discrepancy between the numerical results of Fischer-Cripps[22] and the experimental results of Lim and Chaudhri.[23]

III. SAMPLE SIZE EFFECT AND INDENTER SIZE EFFECT ON THE INDENTATION LOAD–DISPLACEMENT CURVE

To reconcile the apparent difference between the numerical results of Fischer-Cripps[22] and the experimental results of Lim and Chaudhri,[23] we further examined the experimental procedure in Ref. 23 and the numerical model in Ref. 22, as well as the model used in Sec. II. The difference may be due to two possibilities: (i) the assumption of the material constitutive response was incorrect; and/or (ii) the geometrical relationships (i.e., sample size effects and/or indenter size effects) come into play. In both interpreting the experimental results in Ref. 23 and performing the numerical simulations in Sec. II, the material response was assumed to be linearly elastic, and the viscoelasticity and nonlinear elasticity (i.e.,
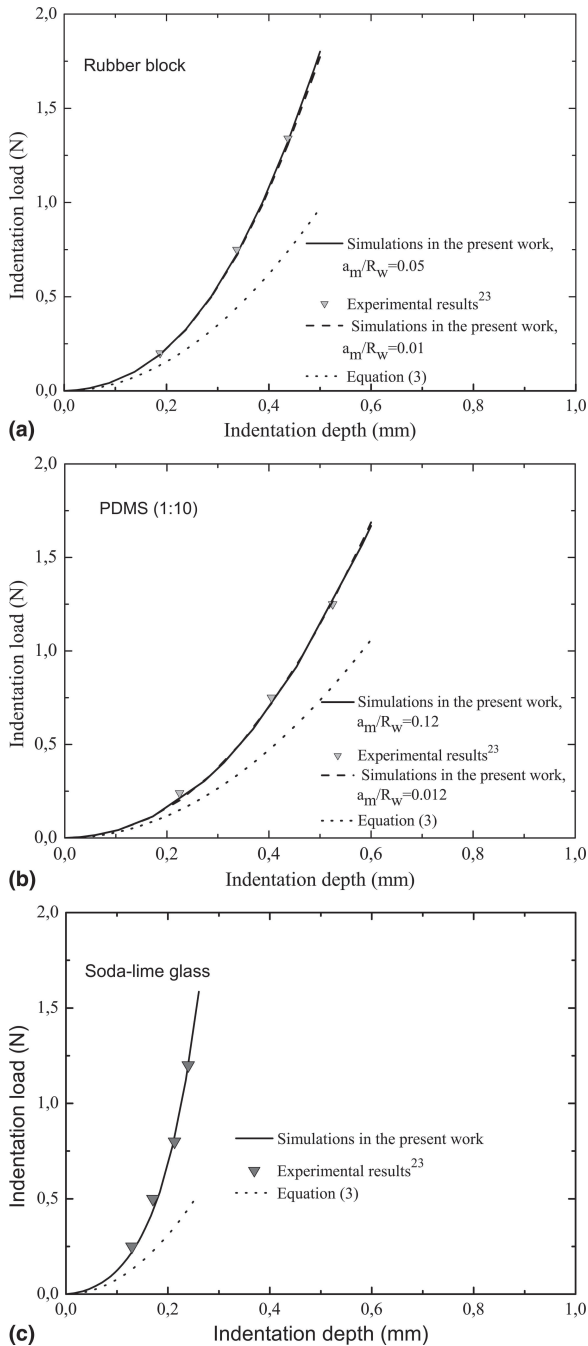
(a)

(b)

(c)

FIG. 3. Comparison of the indentation loading responses obtained from finite element analysis with those given by the experiments in Ref. 24 and Eq. (3) for the rubber cone with the half-apex angle of 75° (a) loading on the rubber block, (b) loading on the PDMS (1:10), and (c) loading on the soda-lime glass.

hyperelasticity) were regarded as being negligible. Lim and Chaudhri[31] confirmed that viscoelastic effects on the indentation loading curve for the experimental materials studied by Lim and Chaudhri[23] were not observed, and the linear elastic assumption of the material response is reliable. Therefore, in the present work, the geometrical factors were examined carefully.

A. Sample size effect

Recently, Xu and Li[32] systematically investigated the indentation sample size effect. They showed that a critical ratio of the indent size to sample size exists, beyond which a significant sample size effect may occur. In the experiments of Lim and Chaudhri,[23] for the rubber indenter indenting into the rubber block and the polydimethylsiloxane (PDMS) substrate, the ratios of the maximum contact radius, a_m, to the sample size parameter, R_w, are about 0.05 and 0.12, respectively, which are larger than the critical values reported by Xu and Li.[32] Thus, sample size effects may come into play. To clarify this issue, we simulated the rubber indenter indenting into the rubber block and PDMS substrate with $R_w = L_h$, and the ratios of a_m/R_w were 0.01 and 0.012, respectively. For these two small a_m/R_w ratios, the sample size effect should be negligible according to the analysis in Ref. 32. For the sake of comparison, the computational results with smaller a_m/R_w ratios are also shown in Figs. 3(a) and 3(b) (dashed lines). It should be pointed out that for the rubber indenter indenting into the soda-lime glass, the sample size should not affect the indentation response because the Young's modulus of the soda-lime glass is much larger than that of the rubber indenter (see Table I). From the results in Fig. 3, it can be seen that the sample size effect in the experiments in Ref. 23 is not significant, and thus not the key factor responsible for the large discrepancy between the numerical results in Ref. 22 and the experimental results in Ref. 23.

B. Indenter size effect

In the experiment using a rubber indenter of 75° (θ in Fig. 1) indenting into a rubber half-space performed by Lim and Chaudhri,[23] the height of the indenter described by *L* in Fig. 1 is about 1.34 mm, and the maximum indentation depth is about 0.43 mm. In this case, the maximum indentation depth is not a small value compared with the indenter height *L*. From the numerical model given by Fig. 1 in the work of Fischer-Cripps,[22] it can be seen that the indenter height used in that study appears to be much larger than the maximum indentation depth. Thus, the indenter size effect is likely to be the key factor that leads to large differences between the numerical results[22] and the experimental results[23] when the elastic deformation of the indenter is significant. To verify this issue, we simulated the indentation of ideally sharp rubber indenters of 75° and 70.3° (see Fig. 1 for the definition of θ) into a rubber half-space with $R_w = L_h$. To avoid the sample size effect, the ratio of a_m/R_w is taken to be 0.01. The indenter of 70.3° is investigated here because this specific indenter geometry is often used in simulations (e.g., in Refs. 8–12, 14, 15, and 20) and is regarded as giving the same depth/area ratio[12,20] or quite similar load-depth curves[8] to the standard Berkovich

indenter. In addition, the results reported in Sec. IV are also based on this specific indenter geometry. The indentation load (P) versus the normalized indentation displacement (h/L) curves are plotted in Fig. 4. From the results, it can be seen that when $L \gg h$ (e.g., $h/L < 0.05$), the computational results [solid lines in Figs. 4(a) and 4(c)] are close to the modified Sneddon's solution given by Eq. (3) [dashed lines in Figs. 4(a) and 4(c)]. In addition, we found that when the indentation depth is not a small value compared with the indenter height, the indentation load approaches the value predicted by the Sneddon's solution given by Eq. (4) [see Figs. 4(b) and 4(d)]. This was the phenomenon observed in the experiments of Lim and Chaudhri[23] (i.e., they found that at the maximum indentation depth the rubber indenter with the half-apex angle of 75° behaves as if it were rigid when it was indented into the PDMS substrate; see Fig. 9 in Ref. 23 for detail). This phenomenon may be rationalized as follows. Because the elastic indenter is firmly attached to a "rigid" indenter rod at the upper end, when h/L becomes large, the strong support provided by the rigid rod is more and more significant, and consequently makes the overall indentation response approach the rigid indenter situation.

Based on all the previous analysis, it is evident that the indenter size effect should be responsible for the large discrepancy between the experimental results of Lim and Chaudhri[23] and the numerical results of Fischer-Cripps[22] when the elastic deformation of the indenter is signifi-

cant. The physics behind the present issue is closely related to one of the fundamental assumptions of the Sneddon analytical equations in contact mechanics (i.e., the deformation is assumed to be local and much greater than the deformation in the bulk material remote from the contact region). In most of the previous research,[18–20] the indenter was taken to be rigid; therefore, one only needed to make sure the indented material has the right geometry that is consistent with the assumption previously made (i.e., that the sample size should be large enough compared with the contact depth). Meanwhile, for the present case, the indenter is assumed to be elastic; thus, the fundamental assumption on relative size scales should be enforced for the indenter as well (i.e., as previously stated, the indenter height should be much larger than the indentation depth). Otherwise, the boundary conditions can significantly affect the indentation response.

Hay et al.[20] have addressed the error in the Sneddon's solution[25] induced by the boundary condition applied in the derivation of the analytical load–displacement curve given by Eq. (4). It has been found that only for the case that the radial displacement of the indented material in the contact region equals zero (e.g., the half-apex angle equals to 90° or Poisson's ratio equals 0.5) is the Sneddon's boundary condition used to derive Eq. (4) strictly valid.[20,33] Taking into consideration that in many cases of practical interest (e.g., a standard Berkovich indenter or a cube corner indenter indenting into a material with Poisson's ratio smaller than 0.5) the radial displacement
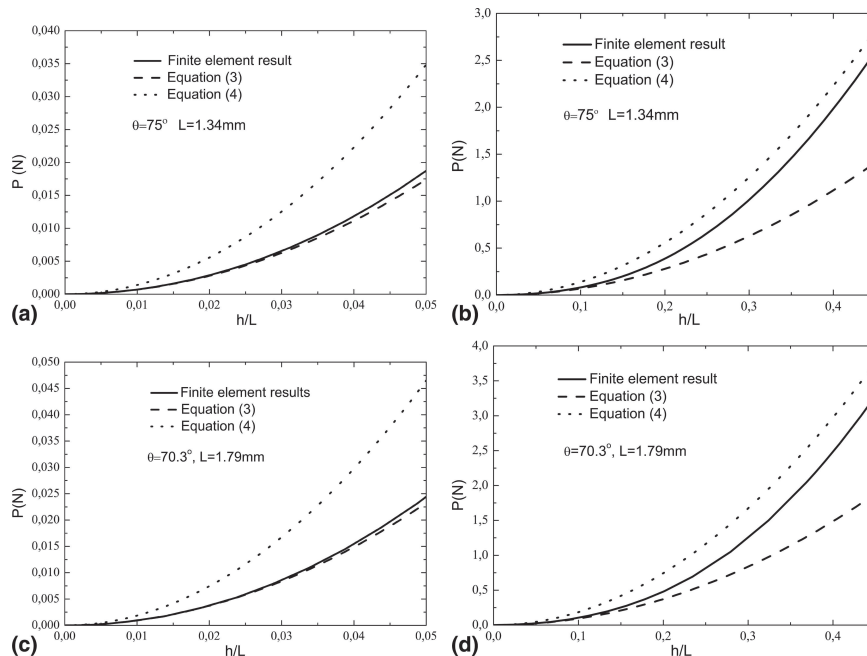

FIG. 4. Comparison of the computational indentation load–displacement curves (solid lines) with the analytical solutions given by Eqs. (3) (dashed lines) and (4) (dotted lines), for the rubber indenters loading on the rubber half-space. (a) 75° indenter and $L \gg h$ (i.e., $h/L < 0.01$); (b) 75° indenter and when h is not a small value compared with the parameter L; (c) 70.3° indenter and $L \gg h$ (i.e., $h/L < 0.01$); and (d) 70.3° indenter and when h is not a small value compared with the parameter L.

of the indented material in the contact region does not disappear, Hay et al.[20] provided correcting factors to Eq. (3) to obtain more accurate results. The corrected Sneddon's solution is thus given by[20]

$$ P = \gamma \, \frac{2}{\pi} \, E^* \, \tan(\theta) h^2 \quad . \tag{8} $$

For the materials with Poisson's ratio $v = 0.3$ and the indenter with $\theta = 70.3°$, $\gamma = 1.067$ in Eq. (8) according to Ref. 20. Moreover, the correcting factors in the work of Hay et al.[20] show that the smaller the half-apex angle is, the larger the correcting factor will be. It should be noted that in the research of Hay et al.,[20] only rigid indenters are considered. However, for the indentation of superhard materials, the elastic deformation of the indenter can be significant. In this case, the problem is more complicated [i.e., not only the Sneddon's boundary condition but also the application of the reduced modulus can lead to errors between Eq. (3) and the real solution]. To highlight the errors induced when using the reduced modulus, we investigated the following critical cases: (i) an elastic indenter of $E = 100$ GPa and $v = 0$, indenting into a rigid surface; and (ii) a rigid indenter indenting into an elastic half-space with $E = 100$ GPa and $v = 0$. For these two cases, the reduced modulus is the same, but the results given by Fig. 5 show that the indentation responses of the two cases are different. According to the analysis above, it is obvious that the correcting factors in the work of Hay et al.[20] would not be applicable to the cases of the indenter exhibiting significant elastic deformation, and new correction factors including the effect of the application of reduced modulus need to be developed. This issue will be addressed in Sec. IV.
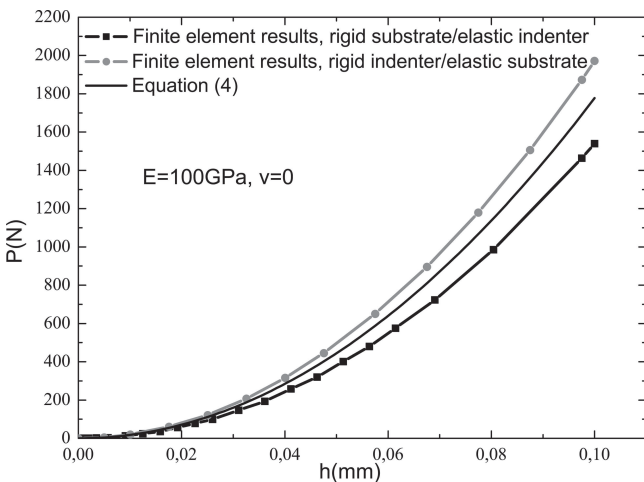

FIG. 5. The indentation load–displacement curves of an elastic indenter with $E = 100$ GPa and $v = 0$ loading on a rigid surface, and a rigid indenter loading on an elastic half-space with $E = 100$ GPa and $v = 0$.

IV. AN EXPLICIT EXPRESSION OF THE INDENTATION LOAD–DISPLACEMENT CURVE FOR A DIAMOND INDENTER INDENTING INTO AN ELASTIC HALF-SPACE

For the case of a conical diamond indenter of 70.3° (i.e., the angle that gives the same depth/area ratio as the standard Berkovich indenter[12,20]) indenting into an elastic half-space with the indenter height being much larger than the indentation depth (a common case in nanoindentation tests), the correction factors to Eq. (3) are explored. For the present issue, for the given loading condition shown in Fig. 1, the correction coefficient γ in Eq. (8) should be a function of the Poisson's ratio v and Young's modulus $E_{material}$ of the indented material, the Poisson's ratio $v_{indenter}$ and Young's modulus $E_{indenter}$ of the indenter, the half-apex angle θ of the indenter, the indentation depth h, and the indenter height L. Therefore, it can be expressed as

$$ \gamma = f(v, E_{material}, E_{indenter}, v_{indenter}, \theta, L, h) \quad . \tag{9} $$

By applying Pi theorem in dimensional analysis,[34,35] Eq. (9) is given by

$$ \gamma = \prod \left(v, \frac{E_{material}}{E_{indenter}}, v_{indenter}, \theta, \frac{h}{L} \right) \quad . \tag{10} $$

For the given half-apex angle $\theta = 70.3°$ and the Poisson's ratio $v_{indenter} = 0.07$ (the diamond indenter is assumed), and when $L \gg h$, Eq. (10) can be reduced as

$$ \gamma = \prod \left(v, \frac{E_{material}}{E_{indenter}} \right) \quad . \tag{11} $$

To make sure the parameter γ is completely independent of the parameter h/L, the ratio of h/L is taken to be 0.01. In the work of Hay et al.,[20] the indenter was assumed to be rigid (i.e., $E_{material}/E_{indenter} \to 0$); therefore, the correction factor in their article is only dependent on the Poisson's ratio of the indented materials. In the present research, the Young's modulus of the diamond indenter is fixed at $E_{indenter} = 1141$ GPa. The Poisson's ratio of the indented material, v, varies from 0 to 0.5. The Young's modulus of the indented material varies from 1 to 1141 GPa (see Table II for detail), leading to $0.00088 \leqslant E_{material}/E_{indenter} \leqslant 1$, which should cover most of the engineering materials (including superhard materials). The diamond indenter tip is studied because it is widely used in indentation experiments (especially when indenting superhard materials). The computational model is the same as that shown in Fig. 1. The maximum indentation depth is taken as 0.01 L. For the material properties listed in Table II, finite element analysis was carried out; the correction coefficients based on systematic computational simulations are given in Fig. 6. According to Fig. 6 and using least squares method, we further obtained the

TABLE II. Elastic properties of materials used in the present computations.

$E_{material}$ (GPa)[a]	$E_{indenter}$ (GPa), $v = 0.07$
1141	1141
1000	1141
500	1141
150	1141
1	1141

[a]For each one of the five cases in the table, Poisson's ratio for the indented material varies from 0.0, 0.3 to 0.5, resulting in a total of 15 different cases.
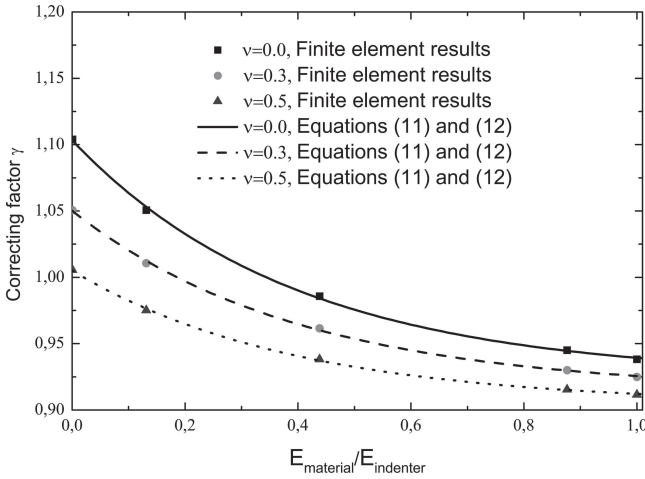

FIG. 6. The relationship between the correction factor γ and the elastic properties of the indented materials (for the case of $h/L < 0.01$, $E_{indenter} = 1141$ GPa, $v_{indenter} = 0.07$, and half-apex angle $\theta = 70.3°$).

explicit expression of the parameter γ given by the following equation and also plotted in Fig. 6 as a comparison.

$$\gamma = C_1(v) + C_2(v)e^{\frac{-\chi}{C_3(v)}} \quad , \tag{12}$$

where $\chi = E_{material}/E_{indenter}$, and

$$C_1(v) = 0.9249 - 0.02737v - 0.02767v^2 \quad , \tag{13a}$$

$$C_2(v) = 0.1784 - 0.1214v - 0.06767v^2 \quad , \tag{13b}$$

$$C_3(v) = 0.3974 + 0.07173v - 0.1647v^2 \quad . \tag{13c}$$

The parameters in Eq. (12) have the following physical meanings:

(i) $C_1 + C_2$ is the same correcting factor as that proposed in the work of Hay et al.,[20] which corrects the errors between Eq. (4) and the real solution that are caused by the Sneddon's boundary for the case of a rigid indenter indenting into an elastic half-space.

(ii) $C_2(1 - e^{-\chi / C_3})$ for a given material reflects the errors induced by the application of the reduced modulus,

which are plotted in Fig. 7 for different material properties. $C_2(1 - e^{-\chi / C_3})$ is obtained as follows. First, for an elastic indenter, A_i, loading into an elastic half-space, B, the real indentation load at a given indentation depth, h_g, is assumed to be $P_{g,T}$. Second, for a rigid indenter, A_r, indenting into an elastic half-space, D, for which the Young's modulus is the combined modulus of the indenter A_i and the elastic substrate B calculated using Eq. (2), and the Poisson's ratio is that of B, the real indentation load at the given indentation depth h_g, which is assumed to be $P_{g,R}$. Third, the indentation load of the elastic indenter A_i loading into B which was predicted using Eq. (3) at the given h_g is assumed to be $P_{g,A}$. The relative error between $P_{g,T}$ and $P_{g,R}$ is defined as $(P_{g,R} - P_{g,T})/P_{g,A}$. According to the results and the previous analysis, it can be determined that $P_{g,R} = (C_1 + C_2)P_{g,A}$ and $P_{g,T} = \gamma P_{g,A}$ with γ given by Eq. (12). Thus, $(P_{g,R} - P_{g,T})/P_{g,A} = C_2(1 - e^{-\chi / C_3})$. From Fig. 7, it can be found that when $E_{material}/E_{indenter} \rightarrow 1$ and for materials with $v = 0$, the application of the reduced modulus will result in an error of 16%.

In the present work, a further verification of the results in Eq. (12) using finite element analysis was performed. A conical diamond indenter of 70.3° indenting into an elastic perfectly plastic superhard material with the Poisson's ratio $v = 0.0$, the Young's modulus $E = 800$ GPa, and the yield strength $\sigma_y = 20$ GPa is analyzed. Fitting the upper 80% of the unloading curve[24] using the power function,[2] the initial unloading slope S is determined. Using S, the maximum indentation load P_m, and the maximum indentation depth h_m as inputs, the Young's modulus is determined from the following procedure.

(i) Taking $\gamma_t = \gamma_0$ (γ_t signifies the true value and γ_0 is the initial value (e.g., $\gamma_0 = 1.034$).

(ii) Using the method of Oliver and Pharr,[2] the reduced modulus can be determined from the following equation.
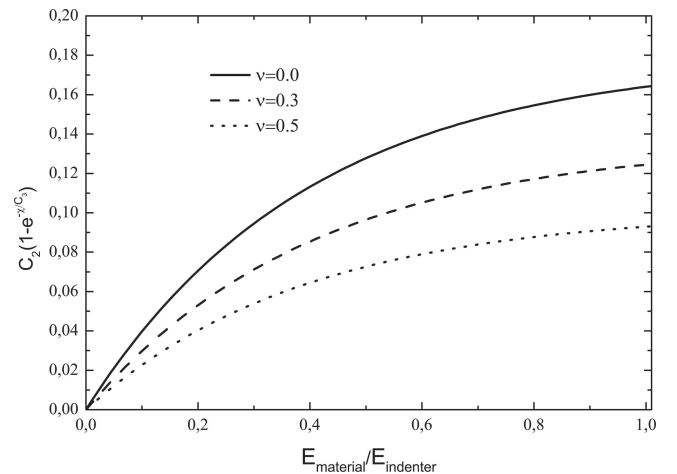

FIG. 7. The errors induced by the application of the reduced modulus, corresponding to different material properties.

$$E^* = \frac{\sqrt{\pi}S}{2\gamma_t \sqrt{A}} \quad , \qquad (14)$$

where A is the project contact area given by

$$A = \pi\left[\tan(\theta)\left(h_m - 0.75\,\frac{P_m}{S}\right)\right]^2 \quad . \qquad (15)$$

(iii) According to the reduced modulus in Step 2, the Young's modulus of the material is further obtained from Eq. (2).

(iv) Based on the Young's modulus obtained in Step 3 and the Poisson's ratio of the material from prior knowledge, γ is determined from Eqs. (12) and (13).

(v) Judge if $\|\gamma - \gamma_t\| \le \delta$, where δ is the error tolerance and is taken as 0.001 in the present work. If yes, go to next step; if no, $\gamma_t = \gamma$, go to Step 2.

(vi) When the iteration is over, the Young's modulus obtained in step 3 is taken as the modulus of the material. The value of the Young's modulus extracted from this procedure is 824 GPa, with an error of 3% with respect to the correct value. On the other hand, applying the correction factor proposed by Hay et al.,[20] a value of 640 GPa with an error of −20% is obtained for the Young's modulus. It should be noted that the contact depth in Eq. (15) was derived by following an elastic-contact analysis.[2] For the elastoplastic materials that exhibit pileup under indentation, the method can significantly underestimate the contact depth.[36] While for the case that the indented material exhibits very small pileup or sink-in, Oliver and Pharr[36] pointed out that the contact area given by Eq. (15) matches the true contact area very well. For the indentation into a superhard material, the accuracy of Eq. (15) was first verified in the present research by using the numerical example discussed above. The ratio of the contact area from Eq. (15) to the contact area determined directly from the finite element simulation is 1.02. In the numerical example above in this section, the ratio of the contact depth h_c to the deflection of the substrate at the apex of the indenter h_t is 0.84 (see Fig. 8 for h_c and h_t); thus, the indented material exhibits apparent sink-in. To further examine the accuracy of Eq. (15) in the case that the sink-in of the substrate is more significant, we simulated the diamond indenter indenting into a material for which the Poisson's ratio is $\nu = 0.0$, the Young's modulus is $E = 800$ GPa, and the yield strength is $\sigma_y = 100$ GPa. In this case, the h_c/h_t ratio is 0.66. The error between the contact area from Eq. (15) and that directly obtained from the finite element simulation is 3.7%. In a recent article, Fischer-Cripps et al.[24] performed an interesting experiment by indenting a diamond indenter into an industrial diamond substrate. Using the method of Oliver and Pharr,[2] they obtained a quite reasonable result for the Young's modulus of the diamond substrate. This result also confirms that Eq. (15) works well for the analysis of the indentation into superhard materials.

In the work of Fischer-Cripps et al.,[24] a correction factor of 1.034 was used in Eq. (14), which is from King.[37] The correction factors reported by King[37] aim at including the effect of non-axisymmetric geometries; it is 1.034 for a triangular punch. Based on a comprehensive analysis, Vlassak and Nix[38] argued that the indentation modulus for a triangular punch is 5.8% higher than that for the axisymmetric punch (i.e., a correction factor of 1.058 is presented for the Berkovich indenter). For the diamond indenter indenting into the diamond half-space, the correction factor according to the present work [Eq. (11)] is smaller than that given by King.[37] But it should be pointed out that the present analysis is limited to the axisymmetric indenter; further investigation on the effect of non-axisymmetric geometries for the deformable indenter shall be useful and will be performed in the near future.

Here, it should be emphasized that the explicit results given by Eqs. (11) and (12) are only valid for the diamond indenter of 70.3°, with a Poisson's ratio of $\nu_{\text{indenter}} = 0.07$, indenting into an elastic half-space with a Young's modulus smaller than 1141 GPa and an $h/L < 0.01$. We also examined the dependence of the correcting factor γ on the parameter h/L (i.e., the correcting factors $\gamma_{0.02}$ and $\gamma_{0.05}$ corresponding to $h/L < 0.02$ and $h/L < 0.05$, respectively, are investigated). We found that the absolute value of the relative difference between $\gamma_{0.01}$ corresponding to an h/L of <0.01 (given by Fig. 6) and $\gamma_{0.02}$ [i.e., $\|(\gamma_{0.01} - \gamma_{0.02})/\gamma_{0.01}\|$ is smaller than 1%, while $\|(\gamma_{0.01} - \gamma_{0.05})/\gamma_{0.01}\|$ is smaller than 3.5%]. This means that the results given by Eqs. (12) and (13) can be used for larger ratios of h/L. In addition, the extension of the present analysis to other indenters can be carried out following a procedure similar to that used in this study. We found that for the indenters with other half-apex angles, when $E_{\text{material}}/E_{\text{indenter}} \to 1$ the application of the reduced modulus in Eq. (3) also leads to significant errors [see Item 2 below Eq. (13) for the definition of the error]. For example, for the indented materials with $\nu = 0$, the maximum error is about 25% for the 60° indenter; and for the 42.28° indenter (equivalent to a cube corner
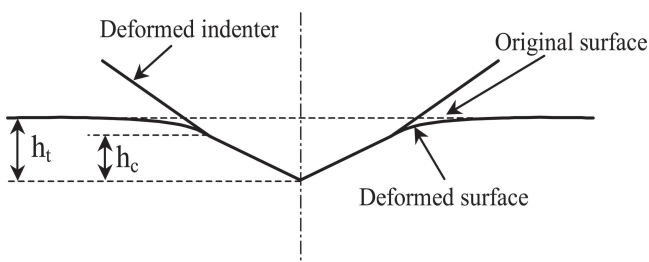

FIG. 8. A schematic drawing of a diamond indenter indenting into a superhard substrate; h_t and h_c represent the deflection of the substrate at the apex of the indenter and the contact depth, respectively.

indenter[20]), the largest error is about 40%. Therefore, one should be cautious in using the correction relationships given in the work of Hay et al.[20] to analyze the nanoindentation data of superhard materials because the effect of deformation of the indenter was not included.

V. CONCLUSIONS

Sneddon's solution[25] of a rigid indenter indenting into an elastic half-space is the basis of the classic method of Oliver and Pharr[2] in the analysis of nanoindentation data to determine the Young's modulus and the hardness of materials. To include the effect of the elastic deformation of the indenter, in the method of Oliver and Pharr,[2] the reduced modulus is applied; however, controversy arose recently for this common practice.[21–24] The present work is a further investigation on an elastic indenter indenting into an elastic half-space that aims to reconcile some apparent inconsistencies found in the literature and provides a more accurate method in extracting mechanical properties for superhard materials using a conical indenter of 70.3°. In summary, the following contributions have been made.

First, the experiments carried out by Lim and Chaudhri[23] have been simulated in detail, and the experimental results and numerical solutions match each other.

Second, the present analysis shows that the indenter size effect is the key factor that is responsible for the large discrepancy between the numerical results of Fischer-Cripps[22] and the experimental results of Lim and Chaudhri.[23] When the elastic deformation of the indenter is significant, the indenter size effect is negligible under the condition of $L \gg h$, the indentation load-displacement curve for the indenter of 70.3° is close to the modified Sneddon's solution[2] [Eq. (3)], as shown in the analysis of Fischer-Cripps.[22] While in the case that the indenter size effect is significant, the indentation response can largely deviate from the modified Sneddon's solution,[2] as observed in the experiments of Lim and Chaudhri.[23]

At last, to accurately extract the mechanical properties of superhard materials using the method of Oliver and Pharr,[2] much attention should be paid to two aspects when the deformation of the indenter is significant. The first important factor is that the indenter size effect as studied in Sec. III should be avoided (i.e., the condition of $L \gg h$ should be satisfied). Another important aspect is the use of the correcting factor γ. Both the Sneddon's boundary condition, as shown in the research of Hay et al.,[20] and the application of the reduced modulus will induce errors that should be included in the corrections to Eq. (3). In the present work, we numerically constructed the explicit expression of the indentation load–displacement curve of a diamond indenter of 70.3° indenting into elastic surfaces. When the Young's modulus of the indenter is much larger than that of the indented material, the present result degenerates to the ones proposed in the work of Hay et al.[20]; whereas, when the deformation of the indenter is significant, the new result presented in this work provides a more accurate evaluation of Young's modulus.

REFERENCES

1. M.F. Doerner and W.D. Nix: A method for interpreting the data from depth-sensing indentation instruments. *J. Mater. Res.* **1,** 601 (1986).
2. W.C. Oliver and G.M. Pharr: An improved technique for determining hardness and elastic modulus using load and displacement sensing indentation experiments. *J. Mater. Res.* **7,** 1564 (1992).
3. D. Tabor: *Hardness of Metals* (Clarendon Press, Oxford, UK, 1951).
4. K.L. Johnson: *Contact Mechanics* (Cambridge University, Cambridge, UK, 1985)
5. J.S. Field and M.V. Swain: Determining the mechanical properties of small volumes of material from submicrometer spherical indentations. *J. Mater. Res.* **10,** 101 (1995).
6. N. Huber and C. Tsakmakis: Determination of constitutive properties from spherical indentation data using neural networks: Part I and II. *J. Mech. Phys. Solids* **47,** 1569 (1999).
7. A.E. Giannakopoulos and S. Suresh: Determination of elastoplastic properties by instrumented sharp indentation. *Scripta Mater.* **40,** 1191 (1999).
8. M. Dao, N. Chollacoop, K.J. Van Vliet, T.A. Venkatesh, and S. Suresh: Computational modelling of the forward and reverse problems in instrumented sharp indentation. *Acta Mater.* **49,** 3899 (2001).
9. J.L. Bucaille, S. Stauss, E. Felder, and J. Michler: Determination of plastic properties of metals by instrumented indentation using different sharp indenters. *Acta Mater.* **51,** 1663 (2003).
10. N. Chollacoop, M. Dao, and S. Suresh: Depth-sensing instrumented indentation with dual sharp indenters. *Acta Mater.* **51,** 3713 (2003).
11. M. Mata and J. Alcalá: Mechanical property evaluation through sharp indentations in elastoplastic and fully plastic contact regimes. *J. Mater. Res.* **18,** 1705 (2003).
12. M. Mata and J. Alcalá: The role of friction on sharp indentation. *J. Mech. Phys. Solids* **52,** 145 (2004).
13. Y.P. Cao and J. Lu: A new method to extract the plastic properties of metal materials from an instrumented spherical indentation loading curve. *Acta Mater.* **52,** 4023 (2004).

14. Y.P. Cao and J. Lu: Size-dependent sharp indentation: I and II. *J. Mech. Phys. Solids* **53,** 33 (2005).
15. Y.P. Cao, X.Q. Qian, J. Lu, and Z.H. Yao: An energy-based method to extract plastic properties of metal materials from conical indentation tests. *J. Mater. Res.* **20,** 1194 (2005).
16. T. Chudoba, N. Schwarzer, and F. Richter: Determination of elastic properties of thin films by indentation measurements with a spherical indenter. *Surf. Coat. Technol.* **127,** 9 (2000).
17. R. Saha and W.D. Nix: Effects of the substrate on the determination of thin film mechanical properties by nanoindentation. *Acta Mater.* **50,** 23 (2002).
18. A.E. Giannakopoulos, P.L. Larsson, and R. Vestergaard: Analysis of Vickers indentation. *Int. J. Solids Struct.* **31,** 2679 (1994).
19. P.L. Larsson, A.E. Giannakopoulos, E. Soderlund, D.J. Rowcliffe, and R. Vestergaard: Analysis of Berkovich indentation. *Int. J. Solids Struct.* **33,** 221 (1996).
20. J.C. Hay, A. Bolshakov, and G.M. Pharr: A critical examination of the fundamental relations used in the analysis of nanoindentation data. *J. Mater. Res.* **14,** 2296 (1999).
21. M.M. Chaudhri: A note on a common mistake in the analysis of nanoindentation data. *J. Mater. Res.* **16,** 336 (2001).
22. A.C. Fischer-Cripps: Use of combined elastic modulus in depth-sensing indentation with a conical indenter. *J. Mater. Res.* **18,** 1043 (2003).
23. Y.Y. Lim and M.M. Chaudhri: Experimental investigations of the normal loading of elastic spherical and conical indenters on elastic flats. *Philos. Mag.* **83,** 3427 (2003).
24. A.C. Fischer-Cripps, P. Karvankova, and S. Veprek: On the measurement of hardness of super-hard coatings. *Surf. Coat. Technol.* **200,** 5645 (2006).
25. I.N. Sneddon: The relation between load and penetration in the axisymmetric Boussinesq problem for a punch of arbitrary profile. *Int. J. Eng. Sci.* **3,** 47 (1965).
26. T.A. Friedmann, J.P. Sullivan, J.A. Knapp, D.R. Tallant, D.M. Follstaedt, D.L. Medlin, and P.B. Mirkarimi: Thick stress-free amorphous tetrahedral carbon films with hardness near that of diamond. *Appl. Phys. Lett.* **71,** 3820 (1997).
27. H. Sjostrom, S. Stafstrom, M. Boman, and J.E. Sundgren: Superhard and elastic carbon nitride thin film having fullerene like microstructure. *Phys. Rev. Lett.* **75,** 1336 (1995).
28. S. Veprek, P. Nesladek, A. Niederhofer, F. Glatz, M. Jilek, and M. Sima: Recent progress in the superhard nanocrystalline composites towards their industrialization understanding of the origin of the superhardness. *Surf. Coat. Technol.* **108-109,** 138 (1998).
29. S. Veprek and A.S. Argon: Towards the understanding of the mechanical properties of super- and ultrahard nanocomposites. *J. Vac. Sci. Technol., B* **20,** 650 (2002).
30. ABAQUS: *Theory Manual Version 6.4* (Hibbitt, Karlsson and Sorensen Inc, Pawtucket, RI, 2004).
31. Y.Y. Lim and M.M. Chaudhri: Indentation of elastic solids with rigid cones. *Philos. Mag.* **84,** 2877 (2004).
32. Z.H. Xu and X. Li: Sample size effect on nanoindentation of micro-/nanostructures. *Acta Mater.* **54,** 1699 (2006).
33. G.H. Fu and A.C. Fischer-Cripps: On Sneddon's boundary conditions used in the analysis of nanoindentation data. *J. Mater. Sci.* **40,** 1789 (2005).
34. G.I. Barenblatt: *Scaling, Self-Similarity, and Intermediate Asymptotics* (Cambridge University Press, Cambridge, 1996).
35. Y.T. Cheng and C.M. Cheng: Scaling, dimensional analysis, and indentation measurements. *Mater. Sci. Eng., R* **44,** 91 (2004).
36. W.C. Oliver and G.M. Pharr: Measurement of hardness and elastic modulus by instrumented indentation: Advances in understanding and refinements to methodology. *J. Mater. Res.* **19,** 3 (2004).
37. R.B. King: Elastic analysis of some punch problems for a layered medium. *Int. J. Solids Struct.* **23,** 1657 (1987).
38. J.J. Vlassak and W.D. Nix: Measuring the elastic properties of anisotropic materials by means of indentation experiments. *J. Mech. Phys. Solids* **42,** 1223 (1994).